Vitamin K epoxide reductase contributes to protein disulfide formation and redox homeostasis within the endoplasmic reticulum

Lori A. Rutkevich and David B. Williams
Department of Biochemistry, University of Toronto, Toronto, ON M5S 1A8, Canada

ABSTRACT **The transfer of oxidizing equivalents from the endoplasmic reticulum (ER) oxidoreductin (Ero1) oxidase to protein disulfide isomerase is an important pathway leading to disulfide formation in nascent proteins within the ER. However, Ero1-deficient mouse cells still support oxidative protein folding, which led to the discovery that peroxiredoxin IV (PRDX4) catalyzes a parallel oxidation pathway. To identify additional pathways, we used RNA interference in human hepatoma cells and evaluated the relative contributions to oxidative protein folding and ER redox homeostasis of Ero1, PRDX4, and the candidate oxidants quiescin-sulfhydryl oxidase 1 (QSOX1) and vitamin K epoxide reductase (VKOR). We show that Ero1 is primarily responsible for maintaining cell growth, protein secretion, and recovery from a reductive challenge. We further show by combined depletion with Ero1 that PRDX4 and, for the first time, VKOR contribute to ER oxidation and that depletion of all three activities results in cell death. Of importance, Ero1, PRDX4, or VKOR was individually capable of supporting cell viability, secretion, and recovery after reductive challenge in the near absence of the other two activities. In contrast, no involvement of QSOX1 in ER oxidative processes could be detected. These findings establish VKOR as a significant contributor to disulfide bond formation within the ER.**

Monitoring Editor
Reid Gilmore
University of Massachusetts

Received: Feb 10, 2012
Revised: Mar 28, 2012
Accepted: Apr 5, 2012

INTRODUCTION

The catalysis of disulfide bond formation in newly synthesized proteins and the subsequent rearrangement of incorrect disulfides are important functions of the endoplasmic reticulum (ER). These reactions are catalyzed by a large family of proteins known as protein disulfide isomerases (PDIs), each of which contains at least one thioredoxin domain (for review see Ellgaard and Ruddock, 2005). Enzymatic action is centered at the catalytic motif, CXXC, and involves disulfide transfer between enzyme and substrate. When net oxidation of the substrate is carried out, the active-site CXXC shuttles from an oxidized disulfide state to a dithiol state as the disulfide is donated to the substrate protein (Hatahet and Ruddock, 2009). For the PDI family member to catalyze another oxidation reaction, the active site must be reoxidized to the disulfide state. The enzymes responsible for carrying out this reoxidation have been the subject of much study over the last decade.

Although in vitro data showing the efficient oxidation of PDI by oxidized glutathione (GSSG) initially suggested that this small molecule was responsible for regenerating oxidized PDI (Lyles and Gilbert, 1991a), they did not explain the ultimate source of oxidizing equivalents to the ER. The discovery of ER oxidoreductin (Ero1p) in yeast solved this problem, as it was shown to be essential for disulfide bond formation (Frand and Kaiser, 1998; Pollard *et al.*, 1998), accepting oxidizing equivalents from molecular oxygen via its bound FAD (Tu and Weissman, 2002; Gross *et al.*, 2004) and oxidizing PDI rather than newly synthesized proteins or small molecules like reduced glutathione (GSH; Tu *et al.*, 2000; Gross *et al.*, 2006; Sevier and Kaiser, 2006). The mammalian isoforms of Ero1p—Ero1α (Cabibbo *et al.*, 2000) and Ero1β (Pagani *et al.*, 2000)—have also been shown to carry out this function, oxidizing PDI and possibly other PDI family members such as ERp57 and ERp72 (Jessop *et al.*,

This article was published online ahead of print in MBoC in Press (http://www.molbiolcell.org/cgi/doi/10.1091/mbc.E12-02-0102) on April 11, 2012.

Address correspondence to: David B. Williams (david.williams@utoronto.ca).

Abbreviations used: Alb, albumin; DTT, dithiothreitol; Ero1, ER oxidoreductin; GSH, reduced glutathione; GSSG, oxidized glutathione; NEM, *N*-ethylmaleimide; PDI, protein disulfide isomerase; PRDX4, peroxiredoxin IV; QSOX1, quiescin-sulfhydryl oxidase 1; UPR, unfolded protein response; VKOR, vitamin K epoxide reductase.

2009; Appenzeller-Herzog *et al.*, 2010; Schulman *et al.*, 2010). Both yeast and mammalian Ero1 are negatively regulated by intramolecular disulfide bonds that are controlled by the availability of reduced PDI; as the levels of reduced PDI increase, the regulatory disulfides are cleaved and Ero1 is activated (Sevier *et al.*, 2007; Baker *et al.*, 2008; Wang *et al.*, 2011). Presumably, this regulation limits the production of potentially toxic H_2O_2 that results from the Ero1-catalyzed reduction of oxygen.

Given that Ero1p function in yeast is essential, it was surprising not only that combined Ero1α- and Ero1β-deficient mice were viable, but also that disulfide bond formation occurred normally during immunoglobulin M assembly and was only partially impaired during insulin biogenesis (Zito *et al.*, 2010b). Furthermore, when Ero1αβ-deficient fibroblasts were exposed to a strong reductive challenge, recovery of ER redox homeostasis exhibited only a modest delay compared with wild-type cells (Appenzeller-Herzog *et al.*, 2010). These findings suggest the existence of Ero1-independent pathways for the formation of disulfide bonds, and several candidates have been proposed, which are defined by their central enzymes: peroxiredoxin IV (PRDX4), quiescin-sulfhydryl oxidase (QSOX1), and vitamin K epoxide reductase (VKOR; reviewed in Bulleid and Ellgaard, 2011).

The pathway involving PRDX4 uses hydrogen peroxide generated by Ero1 or other activities (Tavender and Bulleid, 2010) to oxidize an active-site cysteine to sulfenic acid, which then reacts with a cysteine on another subunit to form an interchain disulfide bond (Cao *et al.*, 2011). This disulfide bond can be donated to thioredoxin domain–containing proteins such as the PDIs. In vitro studies have shown that some, but not all, PDI family members can be oxidized by PRDX4 (Tavender *et al.*, 2010) and that PRDX4 is capable of catalyzing RNaseA oxidative folding in an H_2O_2- and PDI-dependent manner (Zito *et al.*, 2010b). In vivo evidence supports these observations, as shown by the ability of mammalian PRDX4 to rescue the lethality of Ero1p deficiency when expressed in a temperature-sensitive Ero1p mutant yeast strain (Zito *et al.*, 2010b). Furthermore, depletion of PRDX4 by RNA interference exacerbated the phenotype of Ero1α+β–null mouse embryo fibroblasts, resulting in decreased cell growth, hypersensitivity to reducing agents, a more reduced ER redox balance, and impaired collagen secretion (Zito *et al.*, 2010b). Like mammalian Ero1, PRDX4 is not essential, since PRDX4-knockout mice are viable and fertile (Iuchi *et al.*, 2009).

The QSOX1 and VKOR pathways are less well characterized. Mammalian QSOX1 exists in two forms—QSOX1a and QSOX1b—which are the products of differentially spliced QSOX1 RNA (Kodali and Thorpe, 2010). The larger QSOX1a possesses a potential C-terminal transmembrane domain, whereas QSOX1b lacks this domain. Both isoforms contain two thioredoxin domains linked to an Erv2-like domain that possesses oxidase activity. Like Ero1, QSOX1 is a flavoprotein that couples the formation of disulfide bonds to the reduction of molecular oxygen to produce H_2O_2 (Kodali and Thorpe, 2010). However, whereas Ero1 oxidizes PDIs, in vitro studies have shown that QSOX1 shuttles disulfides from its Erv2 domain to one of its thioredoxin domains and then to a broad range of substrates ranging from dithiothreitol (DTT), to GSH, to reduced proteins (Hoober *et al.*, 1996, 1999; Kodali and Thorpe, 2010). In vivo evidence for QSOX1 activity comes primarily from its ability to complement the Ero1 deletion when overexpressed in yeast (Chakravarthi *et al.*, 2007). Physiological substrates for QSOX1 have not yet been identified in mammals. Overexpressed QSOX1 localizes mainly to the Golgi apparatus in Chinese hamster ovary cells, but there may be sufficient levels in the ER at steady state to catalyze disulfide formation in PDIs or folding proteins (Chakravarthi *et al.*, 2007).

Human VKOR is an ER membrane protein that catalyzes the reduction of vitamin K epoxide to vitamin K hydroquinone, a cofactor important for γ-carboxylation of glutamate residues in proteins such as blood-clotting factors (Jin *et al.*, 2007). In this process, a CXXC motif within VKOR is oxidized (Wajih *et al.*, 2005). Conflicting topology models had placed the VKOR CXXC motif either in the cytosol or ER lumen, and it was only recently that its luminal location was definitively demonstrated, thereby raising the possibility that oxidized VKOR could donate a disulfide to PDI family members (Li *et al.*, 2010; Schulman *et al.*, 2010). Indeed, using an in vitro microsomal system, it was shown that VKOR-coupled oxidation of RNaseA was dependent on the presence of PDI and that a complex containing VKOR and PDI could be detected (Wajih *et al.*, 2007). Subsequent substrate-trapping experiments suggested that other members of the PDI family, namely TMX, TMX4, and ERp18, are the preferred interaction partners of VKOR (Schulman *et al.*, 2010). However, a direct effect of VKOR on oxidative folding or ER redox status in cells has not been demonstrated.

Our interest in PDI family oxidants stems from previous work in which we assessed the functional relationships among PDI family members using a knockdown approach in human hepatoma cells. We noted that rapid oxidation of several newly synthesized plasma proteins continued even in the combined absence of PDI family members such as PDI itself, ERp57, and ERp72, enzymes that would be expected to accept oxidizing equivalents from Ero1 (Rutkevich *et al.*, 2010). This suggested either that Ero1 oxidizes many other PDI family members as well or that oxidative pathways other than that involving Ero1 are participating, the latter being consistent with the modest phenotypes described for combined Ero1α+β–knockout cells (Zito *et al.*, 2010b). Accordingly, we decided to assess the contributions of candidate ER oxidant systems to oxidative protein folding in human hepatoma cells by systematically knocking down or inhibiting Ero1α+β, PRDX4, VKOR, and QSOX1 either alone or in combination. The effect of these depletions was monitored by cell growth and viability assays, an assessment of albumin oxidative folding and secretion, determination of oxidized and reduced glutathione levels, and the ability of cells to recover from a reductive challenge. We find that the Ero1 pathway is most vital to oxidative processes within the ER and confirm the participation of PRDX4 as well. Furthermore, we provide the first demonstration that VKOR is a significant contributor to ER oxidation and that it is capable of maintaining cell viability, influencing ER redox balance, and participating in recovery from reductive challenge in the near absence of Ero1 and PRDX4 activities. In contrast, no effect of QSOX1 depletion could be detected.

RESULTS

Both PRDX4 and VKOR support cell growth and viability in the face of Ero1 depletion

To assess the contributions of various oxidative pathways to disulfide formation within the ER, we used an RNA interference (RNAi)–based approach in the human hepatoma cell line HepG2. Ero1α has been reported to be widely expressed throughout mammalian tissues, whereas Ero1β is enriched in pancreas and immunoglobulin-secreting cells (Pagani *et al.*, 2000; Zito *et al.*, 2010a). We detected both isoforms in HepG2 cells (Figure 1A). Similarly, both QSOX1a and QSOX1b were detected, with the predominant species being the smaller QSOX1b isoform. By transfecting cells twice with small interfering RNAs (siRNA) over 6–7 d, we found that Ero1α, Ero1β, PRDX4, QSOX1a/1b, or VKOR could be routinely depleted by 93–98% as determined by Western blot analysis (Figure 1A). This level of knockdown was also achieved when up to three targets were

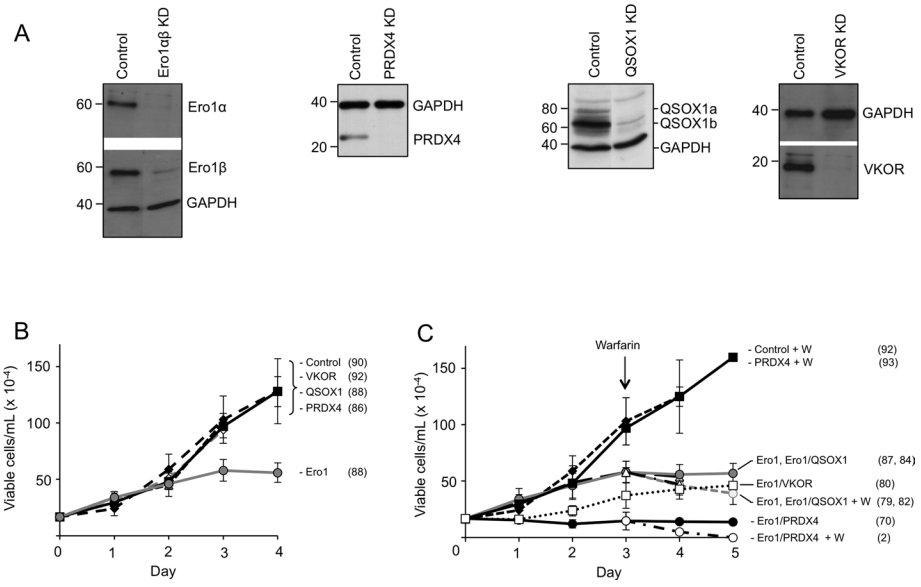

FIGURE 1: Effect of Ero1, PRDX4, QSOX1, and VKOR depletion on cell growth and viability. (A) Candidate ER oxidant enzymes were depleted for 6–7 d in human HepG2 hepatoma cells using siRNA either singly or in combination. Note that a single siRNA targeted both the QSOX1a and QSOX1b isoforms. Equivalent amounts of cell lysates were immunoblotted for the indicated ER enzymes, as well as for GAPDH, which served as an internal loading control. Where two blots are shown, a single blot was stripped and reprobed for the second target. Results are representative of the level of knockdown achieved in both single-target and multitarget siRNA treatment regimes. Numbers refer to molecular weight markers in kilodaltons. (B) HepG2 cell growth and viability were monitored after depletion of a single candidate ER oxidant enzyme (both Ero1α and Ero1β in the case of Ero1). Day 0 is defined as the day of the second transfection with targeting siRNA (day 4 as described in *Materials and Methods*). Targeted enzymes are shown to the right, and average percentage viability on day 4 is indicated in the brackets. Plotted values are averages of three experiments, and error bars represent one SD. (C) Combined depletion of candidate ER oxidant enzymes. Cell growth and viability were monitored daily as described in B. On day 3, cells were treated with 50 μM warfarin to inhibit VKOR activity or DMSO carrier, as indicated by the arrow and "+ W." Cell growth and viability were monitored for another 2 d (except for the PRDX4 and Ero1/QSOX1 knockdowns, which were followed until 4 d only). Bracketed numbers indicate the average viability of recovered cells on day 5.

depleted simultaneously. In some experiments, 50 μM warfarin was used to inhibit VKOR function (Fasco *et al.*, 1983; Rost *et al.*, 2005), since it was determined that overnight treatment with the drug produced similar phenotypes to 7 d of siRNA-mediated VKOR depletion (unpublished data). Furthermore, knockdown of one to three targets resulted in no detectable increase in expression of the ER Hsp70 chaperone BiP nor evidence of Xbp-1 splicing when measured on the final day of knockdown, indicating that an unfolded protein response was not being induced (unpublished data).

Previously, a role for PRDX4 in ER redox homeostasis was revealed upon elimination of the Ero1 pathway in Ero1α+β combined knockout fibroblasts (Zito *et al.*, 2010b). Cells lacking Ero1α+β and depleted of PRDX4 grew more slowly than Ero1α+β–deficient cells, exhibited a more reducing ER, and were more severely impaired in collagen secretion. Consequently, we anticipated that any involvement of PRDX4, VKOR, or QSOX1 in ER redox homeostasis in HepG2 cells would become apparent only upon Ero1α+β depletion. We first examined the effect of individual or combined depletion of oxidative pathways on cell growth and viability. These parameters were monitored for a period of 4–5 d after the last of the two siRNA transfections, as target protein levels declined from 10–17% to trace levels. As shown in Figure 1B, individual knockdown of PRDX4, QSOX1, or VKOR had no effect on cell growth or viability, whereas depletion of Ero1α+β resulted in a significant slowing of growth but no effect on viability (percentage viabilities in brackets). This is in keeping with the substantive role that Ero1 plays in ER oxidative processes (Frand and Kaiser, 1998; Tien *et al.*, 2008). Subsequent combined pathway depletion revealed the relative abilities of the PRDX4, QSOX1, and VKOR pathways to maintain cell function in the absence of Ero1. Cell growth was essentially arrested when PRDX4 was depleted in combination with Ero1α+β, although viability was only modestly affected (Figure 1C). Of interest, a marked growth defect was also observed when VKOR was depleted in combination with Ero1α+β, but no growth phenotype was observed upon combined QSOX1 and Ero1α+β depletion beyond that of Ero1α+β depletion alone (Figure 1C). These findings are consistent with the previous demonstration that PRDX4 contributes to oxidative folding within the ER (Zito *et al.*, 2010b) and, for the first time, implies a similar role for VKOR but not QSOX1. We also inhibited VKOR function by treating cells on day 3 with warfarin, either alone or in combination with siRNA-mediated depletion of other oxidative pathways, and then monitored growth and viability for the next 2 d (denoted by W in Figure 1C). Control cells treated with warfarin exhibited no evidence of toxicity when monitored for 2 d (Figure 1C, Control + W) or even for periods of up to 7 d (unpublished data). In addition, warfarin did not induce an unfolded protein response (UPR) response as monitored by Xbp-1 splicing or by BiP expression levels (unpublished data). Inhibition of VKOR function with warfarin resulted in a growth phenotype only in the context of Ero1α+β depletion (Figure 1C, Ero1+W); combined impairment of the PRDX4 and VKOR pathways resulted in normal cell growth (Figure 1C, PRDX4+W). Furthermore, warfarin treatment permitted assessment of the effects of combined impairment of the Ero1, PRDX4, and VKOR pathways. A gradual loss of cell viability ensued, consistent with the concept that all three pathways contribute to the essential process of ER oxidation (Figure 1C, Ero1/PRDX4+W). The strong-growth phenotypes and loss of cell viability observed in these experiments also provide assurance that the trace levels of target proteins remaining following knockdown are not sufficient to maintain substantial function.

VKOR contributes to an oxidizing ER environment under conditions of Ero1 and PRDX4 deficiency

To extend these findings more directly to oxidative processes within the ER, we first monitored the secretion of the endogenous HepG2 protein albumin (Alb), since we had previously demonstrated Alb secretion defects when its oxidative folding was impaired through PDI member depletion (Rutkevich *et al.*, 2010). Cells were radiolabeled with [^{35}S]Met and chased for 40 min, Alb was immunoisolated from cell lysate and medium samples, and then the percentage secreted was determined. Figure 2A depicts

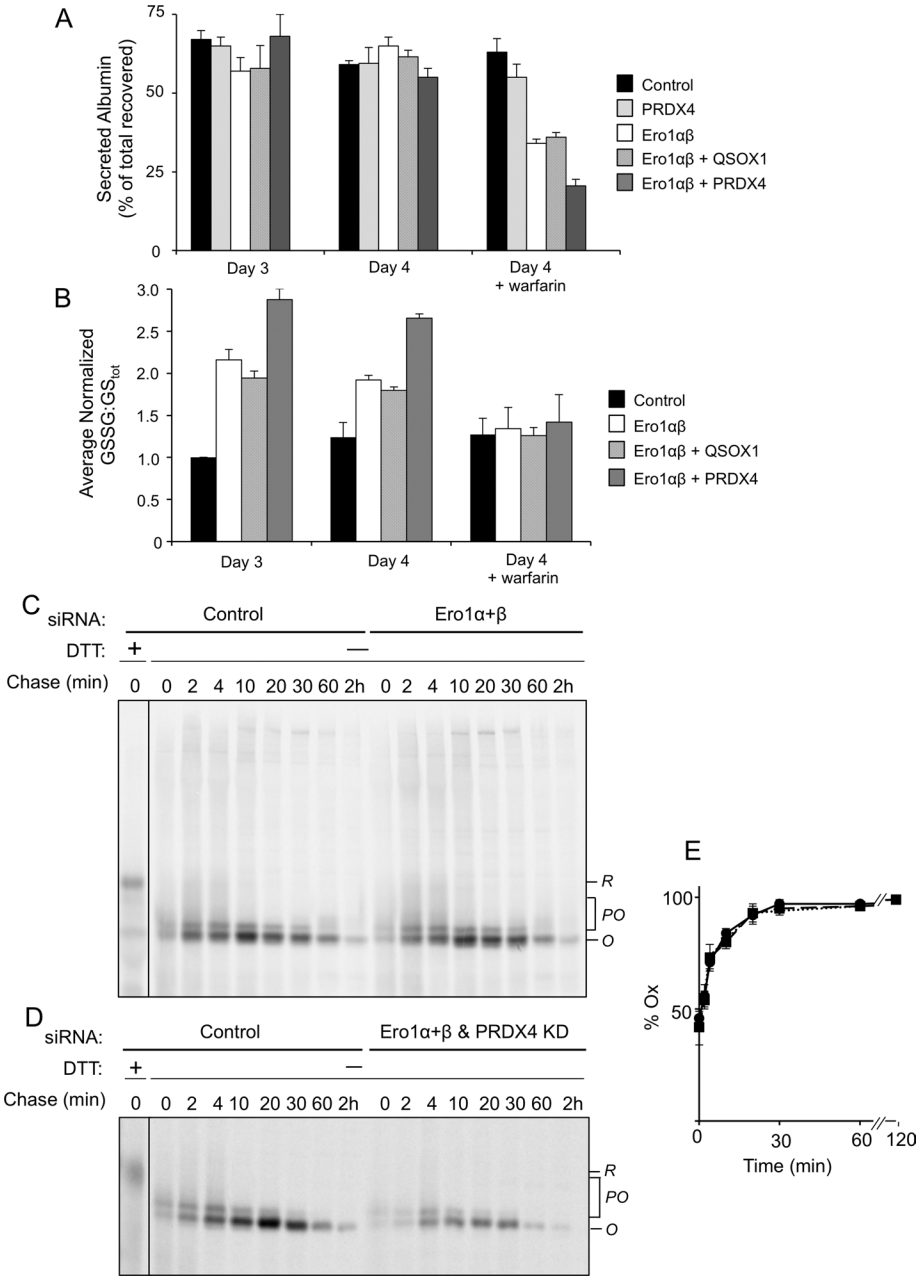

FIGURE 2: Effects of Ero1, PRDX4, QSOX1, and VKOR depletion on the oxidative folding and secretion of albumin and on ER redox environment. HepG2 cells depleted of the indicated candidate ER oxidant enzymes were assessed on days 3 and 4 after the second transfection of siRNAs to monitor changes in (A) albumin secretion and (B) GSSG:GS_{tot} levels. Cells on day 4 were also analyzed after overnight treatment with 50 μM warfarin to inhibit VKOR activity. (A) Albumin secretion was monitored by radiolabeling cells with [^{35}S]Met for 10 min, followed by a chase with excess unlabeled Met for 40 min. Albumin was immunoisolated from cell lysates and chase medium and detected by SDS–PAGE and fluorography. Band intensity was determined by densitometry. Secreted albumin was calculated as a percentage of the total albumin in cell and medium fractions. Results are the mean of two independent experiments, and error bars represent one SD. (B) GSSG and GS_{tot} levels were monitored as described in *Materials and Methods*. Results depict the ratio of GSSG to total GSSG plus GSH (GS_{tot}), normalized to the control day 3 ratio and are the mean of two independent experiments. Error bars represent one SD. (C, D) Kinetics of disulfide formation in albumin. HepG2 cells were treated with control siRNA or the indicated targeting siRNAs and then radiolabeled with [^{35}S]Met for 3 min and chased for the indicated times. After treatment with 20 mM NEM, cells were lysed, and immunoisolated albumin was subjected to nonreducing SDS–PAGE. Shown are fluorograms representative of three independent experiments. The mobilities of reduced (R), partially oxidized (PO), and fully oxidized (O) albumin are indicated. (E) Quantification of gels shown in C and D was carried out using densitometry and by expressing the amount of fully oxidized protein in lysates and media samples as a percentage of the total combined amount of reduced, partially oxidized, and oxidized forms recovered at a given time point. Solid black line, control; dotted black line, Ero1α+β knockdown; dashed black line, Ero1α+β and PRDX4 knockdown. Error bars represent the average of three independent experiments ± one SD.

the results of Alb secretion under various knockdown conditions on days 3 and 4 after the second siRNA transfection and under the same knockdown conditions on day 4 but with the inclusion of warfarin to inhibit VKOR function. Individual pathway depletion through knockdown of Ero1α+β, knockdown of PRDX4, or inhibition of VKOR (control + warfarin) had no effect on Alb secretion. Combinatorial pathway depletions revealed that loss of Ero1α+β plus PRDX4, Ero1α+β plus QSOX1, or PRDX4 plus VKOR did not affect Alb secretion. However, the combined loss of Ero1α+β plus VKOR did result in a modest reduction in secretion. Furthermore, additional depletion of the PRDX4 pathway in combination with Ero1α+β plus VKOR resulted in an even greater defect in Alb secretion. This contrasts with the lack of any additional defect when QSOX1 was depleted in combination Ero1α+β and VKOR. Collectively, these findings suggest that Ero1, PRDX4, and VKOR, but not QSOX, are involved in supporting the oxidative folding and secretion of Alb. Particularly noteworthy was the finding that Alb secretion was normal upon simultaneous depletion of the Ero1 plus PRDX4 pathways but became markedly impaired upon additional inhibition of VKOR with warfarin (Figure 2A; compare Ero1αβ + PRDX4 with Ero1αβ + PRDX4 + warfarin). This suggests that VKOR is an important contributor to the maintenance of ER redox homeostasis upon combined depletion of the Ero1 and PRDX4 pathways.

As an additional means to monitor the consequences of oxidative pathway depletion/inhibition on ER redox homeostasis, we used a colorimetric assay to determine the ratio of GSSG, which originates mainly from the ER (Hwang *et al.*, 1992; Banhegyi *et al.*, 1999), to total cellular glutathione (GS_{tot}, comprised of GSH and GSSG). As shown in Figure 2B, days 3 and 4, depletion of the Ero1α+β pathway resulted in a higher GSSG:GS_{tot} ratio when compared with control cells, reflecting a more oxidizing environment. This seemingly paradoxical finding was noted before (Appenzeller-Herzog *et al.*, 2010) and presumably reflects the compensatory action of other oxidative

pathways to increase the pool of GSSG when the Ero1 pathway is impaired. The increased GSSG pool could potentially reoxidize PDI family members in the absence of Ero1 activity (Lyles and Gilbert, 1991b; Karala *et al.*, 2009; Appenzeller-Herzog, 2011). No further alteration in GSSG:GS_{tot} ratio was observed when QSOX1 was depleted in combination with Ero1α+β, but an even greater increase in ratio was observed upon combined PRDX4 and Ero1 depletion. Of particular interest was the finding that warfarin treatment abolished the observed increases in GSSG:GS_{tot} ratio, thereby implicating VKOR as the source of the compensatory oxidative activity (Figure 2B, day 4 + warfarin).

To assess the contributions of ER oxidant enzymes directly on substrate-level oxidation, we monitored the kinetics of Alb disulfide formation. Cells were subjected to pulse-chase radiolabeling with [^{35}S]Met, treated with *N*-ethyl maleimide (NEM) to alkylate free thiols, and then immunoisolated. Alb was analyzed by nonreducing SDS–PAGE. In control cells (Figure 2C, left), Alb was rapidly converted during the 3-min pulse from its reduced (R) form to more rapidly migrating, partially oxidized (PO) species as well as fully oxidized Alb (O). During the subsequent chase, the various partially oxidized species were gradually converted into the fully oxidized form. On depletion of Ero1α+β (Figure 2C, right), very rapid oxidation of Alb was also observed during the 3-min pulse period and, in fact, there was no observable defect in the overall kinetics of Alb oxidation (quantified in Figure 2E). This is consistent with previous observations using combined Ero1α+β–knockout cells (Zito *et al.*, 2010a, 2010b) and also with the mild to absent phenotypes observed in the cell growth and Alb secretion assays, respectively (Figures 1C and 2A).

To test the involvement of additional oxidative pathways, we next depleted PRDX4 in combination with Ero1α+β (Figure 2D, right). Remarkably, there was no evidence of impaired albumin oxidation as a consequence of this triple depletion. This was surprising, given the growth arrest that accompanies these conditions (Figure 1B) and the strong perturbations in redox balance and secretion observed by others when PRDX4 is depleted in Ero1α+β–knockout mouse fibroblasts (Zito *et al.*, 2010b). However, our findings are consistent with the lack of effect of combined Ero1α+β and PRDX4 depletion on Alb secretion (Figure 2A) and may reflect the compensatory increase in GSSG:GS_{tot} ratio that occurs under these conditions (Figure 2B). Efforts to evaluate the participation of the VKOR pathway in maintaining Alb oxidative folding under conditions of combined Ero1α+β and PRDX4 depletion were hampered by the toxicity observed when warfarin was added to the cells (Figure 1C), limiting the number of cells available for extensive pulse-chase analysis. Consequently, we sought a more sensitive assay to report on substrate level oxidative folding that would permit a clearer assessment of the contributions of each pathway.

The Ero1, PRDX4, and VKOR pathways contribute to recovery after reductive challenge

The technique of treating cells with DTT for a brief period and then washing away the reductant (Braakman *et al.*, 1992) has proven to be a useful tool to monitor the involvement of Ero1 and PDI in the restoration of ER redox homeostasis (Cuozzo and Kaiser, 1999; Mezghrani *et al.*, 2001; Appenzeller-Herzog *et al.*, 2010). Specifically, Appenzeller-Herzog *et al.* (2010) demonstrated that upon DTT washout, restoration of the pretreatment ratios of oxidized:reduced PDI family members and GSSG:GS_{tot} was rapid, and these rapid kinetics depended on both Ero1 and PDI. However, recovery of homeostasis still occurred in the absence of Ero1 or PDI, indicative of the involvement of other oxidant systems. Live-cell imaging studies using a redox-sensitive, ER-localized green fluorescent protein (GFP) confirmed the importance of Ero1α, but not PRDX4, in oxidative recovery after reductive challenge (van Lith *et al.*, 2011).

We extended these analyses by examining the involvement of QSOX1, PRDX4, and VKOR and by monitoring the oxidative folding of Alb as a readout in addition to the GSSG:GS_{tot} ratio. The 8-min treatment with 5 mM DTT used in our study permitted full reduction of the ER but was not long enough to induce a UPR (unpublished data). As shown in Figure 3A (top, Control), fully reduced Alb was observed at 0-min chase and then progressed gradually through partially oxidized forms until it became fully oxidized by 15–30 min. Substantial oxidation was apparent even 5 min after DTT washout, reflecting the rapidity of ER reoxidation. On depletion of Ero1α+β, the oxidative folding of Alb was substantially delayed, in keeping with the demonstrated role of Ero1 in restoration of redox homeostasis (Figure 3A, top, Ero1α+β). A discrete band corresponding to fully reduced Alb persisted to 15 min of chase, with the fully oxidized species being detectable only by 30 min and with full oxidation at 60 min. Figure 3A, right, depicts the slower kinetics of disappearance of fully reduced Alb (dashed gray trace) and the slower formation of the fully oxidized species (dashed black trace) under conditions of Ero1α+β depletion. We also noted some high–molecular weight aggregates under both control and knockdown conditions, but much of this material was not resolved to the reduced form upon analysis by reducing SDS–PAGE, and its level was not reproducible between experiments (Figure 3A, bottom). Consequently, it was not included in the quantitative analysis.

We next assayed the oxidation of Alb in cells depleted of PDI, QSOX1, PRDX4, or VKOR (Figure 3B). PDI knockdown generated a delayed Alb oxidation profile that was similar to that observed with Ero1α+β depletion. This is consistent with the role of PDI as a recipient of oxidizing equivalents from Ero1 (Frand and Kaiser, 1999; Benham *et al.*, 2000; Inaba *et al.*, 2010) and with the previous demonstration that both Ero1 and PDI are required for rapid recovery after reductive challenge (Appenzeller-Herzog *et al.*, 2010). However, it was noted that, unlike the situation with Ero1α+β depletion, in which Alb remained for 15 min as a discrete, fully reduced species (Figure 2A), PDI depletion was associated with significant production of partially oxidized Alb over the same period. This is consistent with the idea that PDI is not an essential conduit to Ero1 and that family members other than PDI are able to receive oxidizing equivalents from Ero1 for catalysis of Alb oxidative folding. In contrast to Ero1α+β and PDI, individual depletion of QSOX1 or VKOR showed no differences in the rates of Alb oxidation compared with control cells (Figure 3B, second and fourth panels). However, depletion of PRDX4 resulted in a slight slowing of Alb oxidation (Figure 3B, third panel). This was particularly obvious at the 15-min chase time, for which a clear decrease in the proportion of fully oxidized Alb was apparent. Thus, even in the presence of the Ero1-to-PDI pathway, the most efficient oxidation was observed only when PRDX4 was also present. Given that Ero1 is highly active after reductive challenge (Sevier *et al.*, 2007; Appenzeller-Herzog *et al.*, 2008), the hydrogen peroxide it produces may be used by PRDX4 to contribute significantly to the reoxidation of PDI family members (Tavender *et al.*, 2010; Zito *et al.*, 2010b).

The individual knockdown experiments revealed that Ero1 plays the predominant role in recovery from reductive challenge. Because Ero1 activity may mask the involvement of other oxidative pathways, we next assessed the participation of the PRDX4, QSOX1, and VKOR pathways through combinatorial depletions with Ero1α+β (Figure 4A). In the case of Ero1α+β and QSOX1 combined depletion, no enhanced phenotype beyond that of Ero1α+β depletion

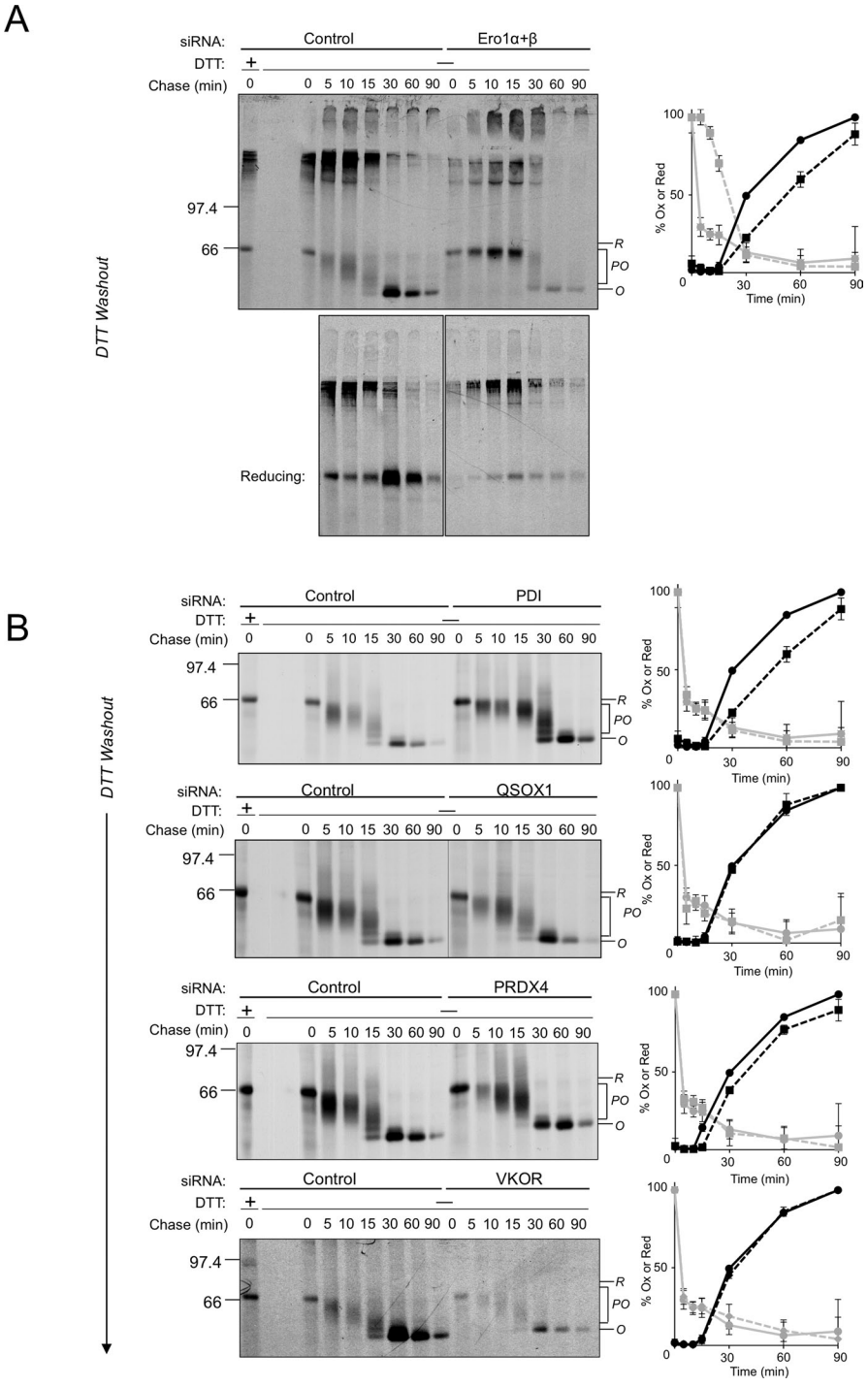

FIGURE 3: Ero1 is the predominant activity responsible for oxidative recovery after DTT treatment. (A) HepG2 cells depleted of Ero1α+β (or control) were treated with 5 mM DTT for 5 min plus an additional 3 min during pulse radiolabeling with [^{35}S]Met. Chase was carried out in the absence of DTT and constituted the "washout" period. NEM treatment, albumin immunoisolation, and analysis were carried out as described in Figure 2, C and D. Top, nonreducing gel; bottom, reducing gel. Right, the quantification of the nonreducing gel. Percentage oxidized albumin (black traces) was determined as described in Figure 2E (solid line, control; dashed line, knockdown). To determine the percentage reduced values (gray traces), the amount of albumin with mobility matching that of the fully reduced control was expressed as a percentage of the total signal recovered at a given time point (solid line, control; dashed line, knockdown). (B) Single knockdowns of the indicated targets were carried out, and radiolabeling with reductive challenge was carried out as described in A. Left, nonreducing gel representative of three independent experiments. Right, quantifications performed as outlined in A . Error bars show the average of three independent experiments ± one SD.

was observed, suggesting that QSOX1 is not a significant participant in recovering from reductive challenge (compare Figures 3A and 4A, top). By contrast, combined depletion of Ero1α+β and PRDX4 resulted in a greater delay in Alb reoxidation than the depletion of Ero1α+β alone (Figure 4A, second panel). Of particular interest was the finding that codepletion of Ero1α+β and VKOR also delayed Alb oxidation to the same or even greater degree than that observed with combined Ero1α+β and PRDX4 depletion (Figure 4A, third panel). This confirms a role for both PRDX4 and VKOR in ER oxidation. Further support for this conclusion comes from combined depletion/inhibition of the PRDX4 and VKOR pathways (Figure 4A, fourth panel). Despite the continued presence of the Ero1/PDI pathway, Alb reoxidation was notably slowed and to a greater extent than that observed upon PRDX4 depletion alone (compare with Figure 3B, third panel).

On the basis of the preceding findings, one would predict that simultaneous loss of the Ero1, PRDX4, and VKOR pathways would have a profound effect on the oxidative recovery of the ER. Unfortunately, due to toxicity issues, we were unable to assess the consequences of inhibiting VKOR in the context of high-efficiency knockdowns of Ero1α+β and PRDX4. As an alternative approach, Ero1α+β and PRDX4 were depleted to ~30% of normal levels and warfarin was added overnight to inhibit VKOR. With this modification, cell death was minimized and pulse-chase analysis after reductive challenge was performed (Figure 4A, bottom). For comparison, the final lane shows the oxidation pattern of Alb after 15 min in the partially depleted cells without warfarin treatment. There is a much greater degree of oxidation of Alb in this final lane when compared with the 15-min time point in the high-efficiency knockdown of Ero1α+β and PRDX4 (Figure 4A, second panel). However, when VKOR was inhibited in the context of the partial Ero1α+β and PRDX4 knockdown, a marked slowing of Alb oxidation was apparent (Figure 4A, bottom; compare 15-min time points without and with warfarin). Once again, this illustrates the significant contribution of VKOR to ER oxidation.

In addition to monitoring substrate level oxidation, we examined the effect of combined pathway depletion on the kinetics of recovery of the GSSG:GS_{tot} ratio to its steady-state level after reductive challenge. For technical reasons, a more rigorous DTT washout protocol was required to obtain reproducible results in this assay. This resulted in more rapid recovery of the ER redox state, which prevented a direct comparison with the kinetics of Alb oxidative folding after DTT washout. Nevertheless, the qualitative effects of pathway depletion can

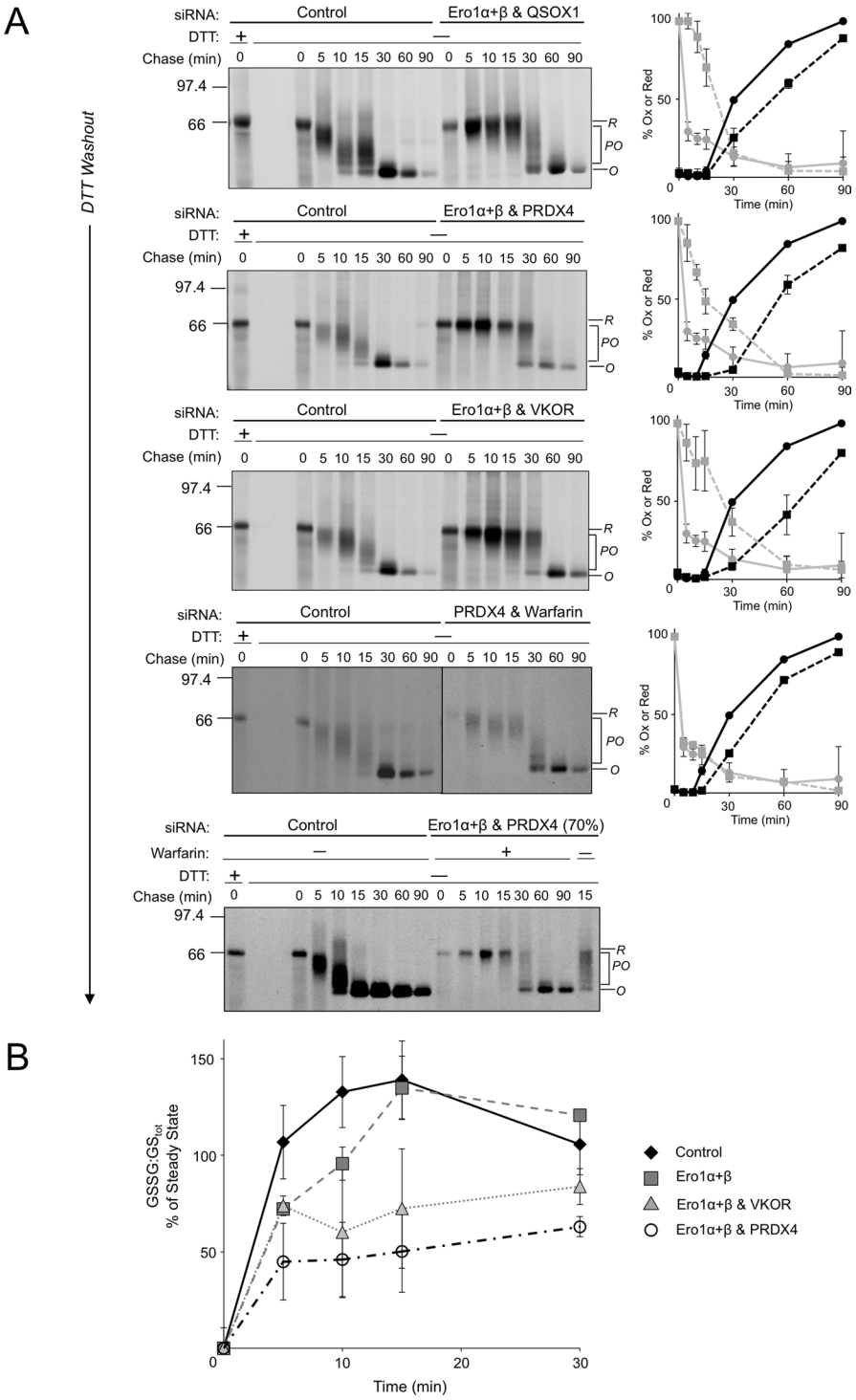

FIGURE 4: Combinatorial knockdowns reveal that PRDX4 and VKOR contribute to recovery after reductive challenge. Codepletions of the indicated enzymes were carried out over 7 d, and then cells were subjected to DTT challenge, followed by quantification of albumin oxidative folding kinetics (A) or GSSG:GS_{tot} ratios (B). For the Ero1α+β and PRDX4 + warfarin experiment (A, bottom), combined depletion was carried out to day 5 posttransfection to obtain ~30% expression of these targets. On day 4, cells were treated with warfarin, and reductive challenge and radiolabeling were performed on day 5. A DMSO-treated sample of knockdown cells at 15 min of chase (last lane) is included for comparison with the 15-min time point of knockdown + warfarin-treated cells. (B) After 8 min of treatment with 5 mM DTT, cells were allowed to recover for the indicated times in DTT-free media and then washed twice with ice-cold PBS and assayed for GSSG and GS_{tot} as described in *Materials and Methods*. The GSSG:GS_{tot} ratio after reductive challenge is quantified as a percentage of the steady-state ratio (independently determined). Averages of three independent experiments (performed in triplicate) are shown ± one SD.

still be compared using both assays. As shown in Figure 4B, under control conditions recovery of the steady-state GSSG:GS_{tot} ratio occurred by 5 min of chase, followed by an overshoot that was corrected by 30 min of chase. In Ero1α+β–depleted cells, recovery of the steady-state GSSG:GS_{tot} ratio was delayed by ~5 min, followed by a similar overshoot and correction by 30 min. This is consistent with previous observations by others (Appenzeller-Herzog *et al.*, 2010). However, we were further able to demonstrate that codepletion of either PRDX4 or VKOR with Ero1α+β results in an even greater impairment in the recovery of steady-state GSSG:GS_{tot} levels, particularly at times exceeding 5 min post washout of the reductant. Thus, like PRDX4, VKOR plays a significant role in oxidative protein folding and the maintenance of ER redox homeostasis.

DISCUSSION

In this investigation, we used a systematic knockdown approach to examine the relative contributions of known and candidate oxidant enzymes to ER redox homeostasis and disulfide bond formation. We confirm that both Ero1 and PRDX4 are important contributors and demonstrate a novel role for VKOR in these processes. However, no phenotypes associated with depletion of QSOX1 could be detected, either in single knockdowns or in combinatorial depletions with other ER oxidants.

Ero1 is essential in both yeast and worms (Frand and Kaiser, 1998; Pollard *et al.*, 1998), but deletion of both Ero1 paralogues in mice generated only mild phenotypes (Zito *et al.*, 2010a). In our studies involving individual depletion of candidate oxidative pathways, we also noted that knockdown of Ero1α+β produced no defects in the oxidative folding or secretion of Alb. However, it was the only pathway that, when depleted individually, resulted in slow cell growth and a substantial delay in recovery of ER redox balance and oxidative folding of Alb after reductive challenge. Furthermore, in combinatorial depletions of candidate pathways, those involving Ero1 were associated with the strongest phenotypes. Collectively, these findings suggest that Ero1 represents the predominant pathway for the de novo generation of disulfide bonds. Although this distinction could be observed, the mild Ero1-depletion phenotype supports the view that other oxidase pathways are acting in parallel to maintain ER redox homeostasis.

Ero1 uses molecular oxygen, producing one molecule of H_2O_2 upon transfer of oxidizing equivalents to PDI (Gross *et al.*, 2006), and the role of PRDX4 in scavenging H_2O_2 to generate disulfide bonds has been well characterized (Tavender and Bulleid, 2010; Tavender

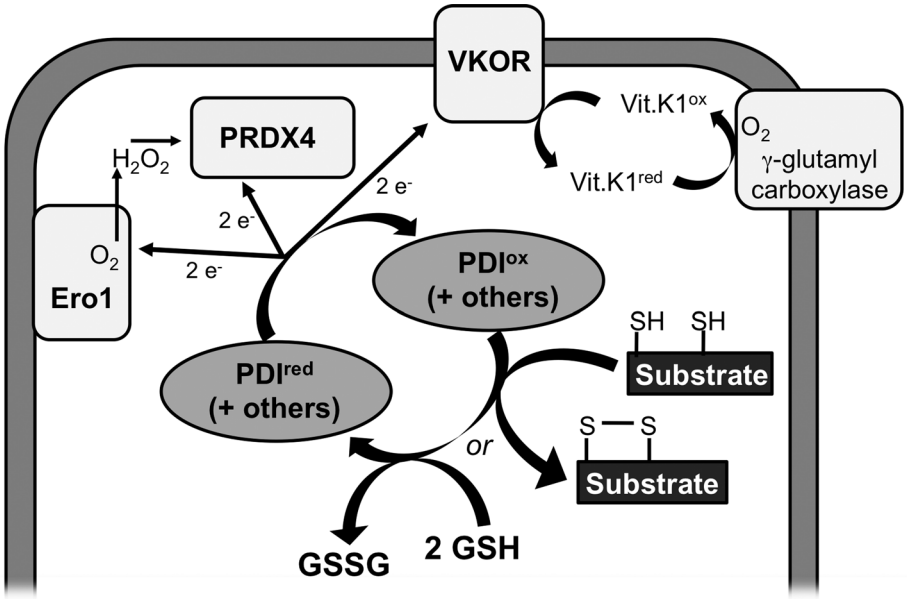

FIGURE 5: Pathways contributing to oxidative protein folding. VKOR, as well as Ero1 and PRDX4, accepts electrons from PDI family members, resulting in the conversion of reduced PDIs (PDI^{red}) to their oxidized forms (PDI^{ox}). PDI^{ox} can catalyze disulfide formation in folding proteins or oxidize glutathione to GSSG. Under conditions when GSSG is abundant, it may also provide oxidizing equivalents for the reoxidation of PDIs.

et al., 2010). Zito *et al.* (2010b) illuminated a key role for PRDX4 in supporting cell growth, secretion, and ER redox homeostasis in mouse embryo fibroblasts lacking Ero1α+β. We confirmed the importance of PRDX4 in human hepatoma cells, since its depletion resulted in a delay in recovery from reductive challenge, even in the presence of Ero1. Furthermore, combined depletion with Ero1 resulted in growth arrest and an even greater delay in recovery from reductive challenge as measured by restoration of oxidized:total glutathione ratio and oxidative folding of Alb. It is striking, however, that under unchallenged conditions, the kinetics of Alb disulfide formation and secretion were normal in the combined absence of Ero1 and PRDX4. This contrasts with the severe secretion defect associated with PRDX4 depletion in Ero1-deficient mouse embryo fibroblasts (Zito *et al.*, 2010b). Furthermore, in the same fibroblasts there was clear evidence of a more reducing ER, yet in HepG2 cells, we observed a more oxidizing ER upon depletion of both pathways. Cumulatively these data suggest that in HepG2 cells an additional oxidative pathway is functioning that is absent or inefficient in mouse embryo fibroblasts.

Given that QSOX1 uses molecular oxygen to generate disulfide bonds, its activity could be sufficient to maintain oxidation in the absence of Ero1 and PRDX4. In our study, depletion of both isoforms of QSOX1 either alone or in combination with Ero1 had no effect on cell growth, oxidized glutathione levels, the kinetics of Alb oxidative folding or secretion, or recovery from reductive challenge. We conclude that at least in human hepatoma cells, QSOX1 does not contribute significantly to ER oxidation. Rather, we discovered that VKOR activity provides the oxidizing power required to maintain ER redox homeostasis in the absence of Ero1 and PRDX4.

In vertebrates, VKOR has a broad tissue distribution that features greatest expression in the liver (Wang *et al.*, 2005; Rost *et al.*, 2009). In contrast, mouse embryos do not express VKOR mRNA at day 7.5 (Ko *et al.*, 1998), and there was only weak expression, sporadically distributed, of VKOR mRNA at day 14.5 (Diez-Roux *et al.*, 2011). These differences in VKOR expression may explain the less-severe phenotype we observed in human hepatoma cells upon combined Ero1 and PRDX4 depletion compared with that reported in mouse embryo fibroblasts (Zito *et al.*, 2010b). Homologues of VKOR have also been reported in some plants, Archaea, and bacteria (Goodstadt and Ponting, 2004). One key feature shared among VKOR homologues is the CXXC motif common in thiol–disulfide exchange reactions. In the case of bacterial VKORs, some homologues cooperate with a periplasmic thioredoxin partner for electron transfer, whereas in others, such as in *Synechococcus* sp., a thioredoxin domain is found on the same polypeptide chain. The crystal structure of this fusion VKOR homologue recently revealed the pathway of electron flow to VKOR from its thioredoxin partner and, of importance, confirmed that topologically this exchange would occur in the ER lumen for mammalian VKOR counterparts (Li *et al.*, 2010).

Wajih *et al.* (2007) first proposed the coupling of the vitamin K cycle to disulfide bond formation via an interaction between VKOR and PDI. These authors reported a decrease in reduced RNaseA-triggered VKOR activity upon PDI knockdown in HEK293 cells or upon inhibition of PDI with bacitracin in rat liver microsomes. Recent work, however, has shown that Cys-43 in the luminal loop of human VKOR preferentially forms mixed disulfides with the membrane-anchored PDI family member TMX and to a lesser extent to TMX4 and ERp18 (Schulman *et al.*, 2010). Although there is debate concerning its PDI family partners, the present work provides the first evidence in intact cells that VKOR contributes to disulfide bond formation and redox homeostasis within the ER. Specifically, the phenotype of combined Ero1 and VKOR depletion was similar to that observed when Ero1 and PRDX4 were depleted, that is, slow growth rate and a prolonged delay in recovering from reductive challenge. Of importance, when both Ero1 and PRDX4 pathways were depleted, VKOR oxidative activity was sufficient to maintain normal kinetics of Alb oxidative folding and secretion and, although delayed, the recovery of redox homeostasis after reductive challenge. Inhibition of VKOR activity in the context of such combined Ero1 + PRDX4 depletion was lethal, suggesting that no other ER oxidative pathway exists in hepatoma cells with sufficient activity to support essential cell functions. Thus, as depicted in Figure 5, the use of VKOR to generate disulfide bonds de novo in the ER represents an important alternative to the Ero1 and PRDX4 pathways. In this pathway, VKOR accepts electrons during oxidation of PDI family members and in the process reduces vitamin K epoxide ($Vit.K1^{ox}$) to the hydroquinone ($Vit.K1^{red}$). The vitamin K hydroquinone is utilized by the ER membrane protein γ-glutamyl carboxylase for the production of γ-carboxyglutamate (Gla) in vitamin K–dependent proteins (reviewed in Presnell and Stafford, 2002). During this reaction, the vitamin K epoxide is regenerated with molecular oxygen serving as the ultimate electron acceptor, producing a molecule of water. Of the 18 known Gla-containing proteins in humans, at least 10 are synthesized in the liver, including seven blood coagulation and anticoagulation factors. This suggests that the γ-glutamyl carboxylase likely has sufficient activity in HepG2 hepatoma cells to support the observed oxidative functions of VKOR.

During the course of these studies, we observed a higher ratio of oxidized:total glutathione in cells depleted of Ero1α+β, in keeping with a previous report (Appenzeller-Herzog *et al.*, 2010). This was further increased upon combined depletion of the Ero1 and PRDX4 pathways. We reasoned that parallel oxidant pathways could be generating oxidized glutathione as one means to support continued disulfide bond formation in compensation for the lack of Ero1 and PRDX4 activities. Of note, inhibition of VKOR activity eliminated the higher levels of oxidized glutathione, consistent with VKOR being a significant source of this oxidative activity. This process is summarized in Figure 5, where VKOR, as well as Ero1 and PRDX4, participates in de novo formation of disulfides via PDI or other PDI family members (PDI^{ox}). Oxidized PDI then passes on oxidizing equivalents to substrate or to reduced glutathione to form GSSG. In the absence of one or more oxidative inputs into PDI, such as loss of Ero1 activity, the remaining oxidative pathways may compensate by driving GSSG formation, as detected by its elevated levels. By shifting the ER glutathione buffer to a higher proportion of GSSG, cells have a greater pool available for the GSSG-driven oxidation of PDIs and the maintenance of substrate oxidation as proposed by Appenzeller-Herzog (2011). The existence of these parallel and compensatory pathways in complex eukaryotes highlights the remarkable complexity associated with maintaining ER redox balance in support of the essential process of disulfide bond formation.

MATERIALS AND METHODS

Cell lines and antibodies

Human hepatoma HepG2 cells were maintained in high-glucose DMEM containing 10% fetal bovine serum and antibiotics. Antibodies used in this study were anti-PDI (Assay Designs, Stressgen, Enzo Life Sciences, San Diego, CA), anti-BiP (BD Biosciences, San Diego, CA), anti–glyceraldehyde-3-phosphate dehydrogenase (GAPDH; Millipore, Billerica, MA), anti-Ero1α and -PRDX4 (Abcam, Cambridge, MA), anti-albumin (Sigma-Aldrich, St. Louis, MO), and anti-QSOX1 (Proteintech Group, Chicago, IL). Rabbit antisera directed against Ero1β (Zito *et al.*, 2010a) and VKOR (Rishavy *et al.*, 2010) were gifts of David Ron (University of Cambridge, Cambridge, United Kingdom) and Kathleen Berkner (Cleveland Clinic, Cleveland, OH), respectively.

RNA interference and VKOR inhibition

For individual target knockdowns, Stealth Select siRNAs (40 nM; Invitrogen, Carlsbad, CA), either specific for Ero1α, Ero1β, QSOX1a/QSOX1b, PRDX4, VKOR, or PDI or a negative nontargeting control, were mixed with 6 µl of Oligofectamine (Invitrogen) and transfected on day 1, and again on day 4, into HepG2 cells, with analysis on day 7 (Rutkevich *et al.*, 2010). For codepletion of Ero1α and Ero1β, cells were treated with a mixture of Ero1α and Ero1β siRNAs on day 1 (20 nM final concentration each) and then only Ero1α on day 4 and only Ero1β on day 5 (40 nM final concentration) for analysis on day 7. When a third target, VKOR or PRDX4, was knocked down, the transfection protocol was carried out as follows: day 1, 20 nM each Ero1α and Ero1β siRNAs; day 2, 40 nM VKOR or PRDX4 siRNA; day 4, 30 nM Ero1α + 20 nM VKOR or PRDX4 siRNA; day 5, 30 nM Ero1β + 20 nM VKOR or PRDX4 siRNA; and analysis on day 7. For the Ero1α+β and QSOX1 knockdown, the transfection protocol used was as follows: day 1, 20 nM each of Ero1α and Ero1β siRNA; day 3, 40 nM QSOX1 siRNA; day 4, 30 nM Ero1α + 10 nM QSOX1 siRNA; day 5, 30 nM Ero1β + 10 nM QSOX1 siRNA; for analysis on day 7. For inhibition of VKOR using warfarin, cells were replated in medium containing 50 µM warfarin (Sigma-Aldrich) dissolved in dimethyl sulfoxide (DMSO) and incubated overnight at 37°C. Control cells were treated with DMSO only. Cell growth and viability were monitored from day 4 onward by trypsinizing and suspending cells in 1.5 ml of medium, counting, and determining percentage of viable cells by trypan blue exclusion.

Pulse-chase radiolabeling, reductive (DTT) challenge, and immunoisolations

For pulse-chase radiolabeling experiments, HepG2 cells in 60-mm dishes were starved for 30 min with Met-free RPMI 1640 and radiolabeled for 3 min in 1 ml of medium containing 0.1 mCi of [^{35}S]Met (>1000 Ci/mmol; PerkinElmer, Waltham, MA). The cells were chased for various durations in RPMI 1640 supplemented with 1 mM Met. The chase was terminated by placing cells on ice, and then free thiols were alkylated by incubating on ice for 3 min in 2 ml of phosphate-buffered saline (PBS) supplemented with 20 mM NEM (Sigma-Aldrich). Cells were then lysed at 4°C in 1 ml RIPA buffer (50 mM Tris, pH 7.4, 150 mM NaCl, 1 mM EDTA, 1% NP-40, 0.25% Na deoxycholate [DOC], 0.1% SDS, and protease inhibitors) containing 20 mM NEM and subjected to immunoisolation with 30 µg of anti-albumin antibody. Media samples collected from 30-min chase times onward were also subjected to immunoisolation. After rocking for 2 h at 4°C, immune complexes were recovered by incubation for 1 h with 30 µl of protein A agarose beads (GE Healthcare, Piscataway, NJ). Bead-bound complexes were washed four times with 50 mM Tris, pH 7.4, 150 mM NaCl, 1 mM EDTA, 0.1% NP-40, 0.025% DOC, and 0.01% SDS. Samples were then split equally for elution in SDS–PAGE sample buffer, either lacking or containing 40 mM DTT, and analyzed by SDS–PAGE (10% gels). Radioactive proteins were detected by fluorography, and band intensities were quantified by scanning x-ray films, followed by densitometric analysis using Quantity One software (Bio-Rad, Hercules, CA).

In experiments coupling pulse-chase radiolabeling with a reductive DTT challenge, HepG2 cells in 60-mm dishes were starved in 2 ml of Met-free RPMI for 25 min, and then 1 ml of Met-free RPMI containing 15 mM DTT (Bioshop, Burlington, Canada) was added per dish (5 mM final DTT concentration) and incubation was continued for another 5 min. Cells were subsequently pulse radiolabeled for 3 min in 1 ml of Met-free media containing 0.1 mCi of [^{35}S]Met and 5 mM DTT. The chase and DTT washout were carried out by removing labeling medium and replacing with 3 ml of medium supplemented with 1 mM Met. Alkylation with NEM, lysis, immunoisolation, and analysis was carried out as described.

For experiments involving the assay of glutathione levels after reductive challenge, cells in 35-mm dishes were treated with 1 ml of medium containing 5 mM DTT for 8 min. The DTT-containing medium was removed, cells were quickly washed with 1 ml of medium lacking DTT, and then cells were incubated with 2 ml of fresh medium for the indicated times.

Glutathione assay

Cellular levels of GSSG and total (oxidized plus reduced) glutathione (GS_{tot}) were quantified using a modified version of the glutathione reductase recycling assay described by Rahman *et al.* (2006). Briefly, after various knockdowns and/or reductive challenge with DTT, HepG2 cells were washed in PBS, scraped from the plate in 40 µl of PBS, transferred into ice-cold microfuge tubes containing 10 µl of 5% 5-sulfosalicyclic acid, and vortexed immediately. After centrifugation at 4°C for 5 min at 12,000 × *g*, the supernatant fraction was transferred to new microfuge tubes and diluted with 330 µl of 0.1 M sodium phosphate buffer, pH 7.4, containing 1 mM EDTA (KPE buffer). To assay GS_{tot}, 50 µl of sample was added directly to the wells of a 96-well plate. To measure GSSG, 130 µl of each

sample was first mixed with 6 µl of 2-vinylpyridine (Sigma-Aldrich), which reacts with GSH selectively, and incubated for 1 h at room temperature. A 50-µl aliquot was then applied to the wells of the 96-well plate. All wells were mixed with 100 µl of reaction mixture (for one plate, freshly prepared: 2.8 ml of 1 mM Ellman's reagent [5,5′-dithiobis(2-nitrobenzoic acid)], 3.75 ml of 1 mM NADPH, 20 U of glutathione reductase, 5.85 ml of KPE buffer; all reagents from Sigma-Aldrich), and absorbance was read continuously at 405 nm for a total of 5 min. Initial reaction rates were compared with those obtained with a standard curve spanning the range from 0 to 500 pmol of GSSG.

ACKNOWLEDGMENTS

We thank David Ron and Kathleen Berkner for the generous gift of antibodies and Myrna Cohen-Doyle for expert technical assistance. We gratefully acknowledge funding for this work from the Canadian Cancer Society and the Canadian Institutes of Health Research.

REFERENCES

Appenzeller-Herzog C (2011). Glutathione- and non-glutathione-based oxidant control in the endoplasmic reticulum. J Cell Sci 124, 847–855.

Appenzeller-Herzog C, Riemer J, Christensen B, Sorensen ES, Ellgaard L (2008). A novel disulphide switch mechanism in Ero1alpha balances ER oxidation in human cells. EMBO J 27, 2977–2987.

Appenzeller-Herzog C, Riemer J, Zito E, Chin KT, Ron D, Spiess M, Ellgaard L (2010). Disulphide production by Ero1alpha-PDI relay is rapid and effectively regulated. EMBO J 29, 3318–3329.

Baker KM, Chakravarthi S, Langton KP, Sheppard AM, Lu H, Bulleid NJ (2008). Low reduction potential of Ero1alpha regulatory disulphides ensures tight control of substrate oxidation. EMBO J 27, 2988–2997.

Banhegyi G, Lusini L, Puskas F, Rossi R, Fulceri R, Braun L, Mile V, di Simplicio P, Mandl J, Benedetti A (1999). Preferential transport of glutathione versus glutathione disulfide in rat liver microsomal vesicles. J Biol Chem 274, 12213–12216.

Benham AM, Cabibbo A, Fassio A, Bulleid N, Sitia R, Braakman I (2000). The CXXCXXC motif determines the folding, structure and stability of human Ero1-Lalpha. EMBO J 19, 4493–4502.

Braakman I, Helenius J, Helenius A (1992). Manipulating disulfide bond formation and protein folding in the endoplasmic reticulum. EMBO J 11, 1717–1722.

Bulleid NJ, Ellgaard L (2011). Multiple ways to make disulfides. Trends Biochem Sci 36, 485–492.

Cabibbo A, Pagani M, Fabbri M, Rocchi M, Farmery MR, Bulleid NJ, Sitia R (2000). ERO1-L, a human protein that favors disulfide bond formation in the endoplasmic reticulum. J Biol Chem 275, 4827–4833.

Cao Z, Tavender TJ, Roszak AW, Cogdell RJ, Bulleid NJ (2011). Crystal structure of reduced and of oxidized peroxiredoxin IV enzyme reveals a stable oxidized decamer and a non-disulfide-bonded intermediate in the catalytic cycle. J Biol Chem 286, 42257–42266.

Chakravarthi S, Jessop CE, Willer M, Stirling CJ, Bulleid NJ (2007). Intracellular catalysis of disulfide bond formation by the human sulfhydryl oxidase, QSOX1. Biochem J 404, 403–411.

Cuozzo JW, Kaiser CA (1999). Competition between glutathione and protein thiols for disulphide-bond formation. Nat Cell Biol 1, 130–135.

Diez-Roux G *et al*. (2011). A high-resolution anatomical atlas of the transcriptome in the mouse embryo. PLoS Biol 9, e1000582.

Ellgaard L, Ruddock LW (2005). The human protein disulphide isomerase family: substrate interactions and functional properties. EMBO Rep 6, 28–32.

Fasco MJ, Principe LM, Walsh WA, Friedman PA (1983). Warfarin inhibition of vitamin K 2,3-epoxide reductase in rat liver microsomes. Biochemistry 22, 5655–5660.

Frand AR, Kaiser CA (1998). The ERO1 gene of yeast is required for oxidation of protein dithiols in the endoplasmic reticulum. Mol Cell 1, 161–170.

Frand AR, Kaiser CA (1999). Ero1p oxidizes protein disulfide isomerase in a pathway for disulfide bond formation in the endoplasmic reticulum. Mol Cell 4, 469–477.

Goodstadt L, Ponting CP (2004). Vitamin K epoxide reductase: homology, active site and catalytic mechanism. Trends Biochem Sci 29, 289–292.

Gross E, Kastner DB, Kaiser CA, Fass D (2004). Structure of Ero1p, source of disulfide bonds for oxidative protein folding in the cell. Cell 117, 601–610.

Gross E, Sevier CS, Heldman N, Vitu E, Bentzur M, Kaiser CA, Thorpe C, Fass D (2006). Generating disulfides enzymatically: reaction products and electron acceptors of the endoplasmic reticulum thiol oxidase Ero1p. Proc Natl Acad Sci USA 103, 299–304.

Hatahet F, Ruddock LW (2009). Protein disulfide isomerase: a critical evaluation of its function in disulfide bond formation. Antioxid Redox Signal 11, 2807–2850.

Hoober KL, Joneja B, White HB 3rd, Thorpe C (1996). A sulfhydryl oxidase from chicken egg white. J Biol Chem 271, 30510–30516.

Hoober KL, Sheasley SL, Gilbert HF, Thorpe C (1999). Sulfhydryl oxidase from egg white. A facile catalyst for disulfide bond formation in proteins and peptides. J Biol Chem 274, 22147–22150.

Hwang C, Sinskey AJ, Lodish HF (1992). Oxidized redox state of glutathione in the endoplasmic reticulum. Science 257, 1496–1502.

Inaba K, Masui S, Iida H, Vavassori S, Sitia R, Suzuki M (2010). Crystal structures of human Ero1alpha reveal the mechanisms of regulated and targeted oxidation of PDI. EMBO J 29, 3330–3343.

Iuchi Y, Okada F, Tsunoda S, Kibe N, Shirasawa N, Ikawa M, Okabe M, Ikeda Y, Fujii J (2009). Peroxiredoxin 4 knockout results in elevated spermatogenic cell death via oxidative stress. Biochem J 419, 149–158.

Jessop CE, Watkins RH, Simmons JJ, Tasab M, Bulleid NJ (2009). Protein disulphide isomerase family members show distinct substrate specificity: P5 is targeted to BiP client proteins. J Cell Sci 122, 4287–4295.

Jin DY, Tie JK, Stafford DW (2007). The conversion of vitamin K epoxide to vitamin K quinone and vitamin K quinone to vitamin K hydroquinone uses the same active site cysteines. Biochemistry 46, 7279–7283.

Karala AR, Lappi AK, Saaranen MJ, Ruddock LW (2009). Efficient peroxide-mediated oxidative refolding of a protein at physiological pH and implications for oxidative folding in the endoplasmic reticulum. Antioxid Redox Signal 11, 963–970.

Ko MS *et al*. (1998). Genome-wide mapping of unselected transcripts from extraembryonic tissue of 7.5-day mouse embryos reveals enrichment in the t-complex and under-representation on the X chromosome. Hum Mol Genet 7, 1967–1978.

Kodali VK, Thorpe C (2010). Oxidative protein folding and the quiescin-sulfhydryl oxidase family of flavoproteins. Antioxid Redox Signal 13, 1217–1230.

Li W, Schulman S, Dutton RJ, Boyd D, Beckwith J, Rapoport TA (2010). Structure of a bacterial homologue of vitamin K epoxide reductase. Nature 463, 507–512.

Lyles MM, Gilbert HF (1991a). Catalysis of the oxidative folding of ribonuclease A by protein disulfide isomerase: dependence of the rate on the composition of the redox buffer. Biochemistry 30, 613–619.

Lyles MM, Gilbert HF (1991b). Catalysis of the oxidative folding of ribonuclease A by protein disulfide isomerase: pre-steady-state kinetics and the utilization of the oxidizing equivalents of the isomerase. Biochemistry 30, 619–625.

Mezghrani A, Fassio A, Benham A, Simmen T, Braakman I, Sitia R (2001). Manipulation of oxidative protein folding and PDI redox state in mammalian cells. EMBO J 20, 6288–6296.

Pagani M, Fabbri M, Benedetti C, Fassio A, Pilati S, Bulleid NJ, Cabibbo A, Sitia R (2000). Endoplasmic reticulum oxidoreductin 1-lbeta (ERO1-Lbeta), a human gene induced in the course of the unfolded protein response. J Biol Chem 275, 23685–23692.

Pollard MG, Travers KJ, Weissman JS (1998). Ero1p: a novel and ubiquitous protein with an essential role in oxidative protein folding in the endoplasmic reticulum. Mol Cell 1, 171–182.

Presnell SR, Stafford DW (2002). The vitamin K-dependent carboxylase. Thromb Haemost 87, 937–946.

Rahman I, Kode A, Biswas SK (2006). Assay for quantitative determination of glutathione and glutathione disulfide levels using enzymatic recycling method. Nat Protocols 1, 3159–3165.

Rishavy MA, Usubalieva A, Hallgren KW, Berkner KL (2010). Novel insight into the mechanism of the vitamin K oxidoreductase (VKOR): electron relay through Cys43 and Cys51 reduces VKOR to allow vitamin K reduction and facilitation of vitamin K-dependent protein carboxylation. J Biol Chem 286, 7267–7278.

Rost S, Fregin A, Hunerberg M, Bevans CG, Muller CR, Oldenburg J (2005). Site-directed mutagenesis of coumarin-type anticoagulant-sensitive VKORC1: evidence that highly conserved amino acids define structural requirements for enzymatic activity and inhibition by warfarin. Thromb Haemost 94, 780–786.

Rost S, Pelz HJ, Menzel S, MacNicoll AD, Leon V, Song KJ, Jakel T, Oldenburg J, Muller CR (2009). Novel mutations in the VKORC1 gene

of wild rats and mice—a response to 50 years of selection pressure by warfarin? BMC Genet 10, 4.
Rutkevich LA, Cohen-Doyle MF, Brockmeier U, Williams DB (2010). Functional relationship between protein disulfide isomerase family members during the oxidative folding of human secretory proteins. Mol Biol Cell 21, 3093–3105.
Schulman S, Wang B, Li W, Rapoport TA (2010). Vitamin K epoxide reductase prefers ER membrane-anchored thioredoxin-like redox partners. Proc Natl Acad Sci USA 107, 15027–15032.
Sevier CS, Kaiser CA (2006). Disulfide transfer between two conserved cysteine pairs imparts selectivity to protein oxidation by Ero1. Mol Biol Cell 17, 2256–2266.
Sevier CS, Qu H, Heldman N, Gross E, Fass D, Kaiser CA (2007). Modulation of cellular disulfide-bond formation and the ER redox environment by feedback regulation of Ero1. Cell 129, 333–344.
Tavender TJ, Bulleid NJ (2010). Peroxiredoxin IV protects cells from oxidative stress by removing H2O2 produced during disulphide formation. J Cell Sci 123, 2672–2679.
Tavender TJ, Springate JJ, Bulleid NJ (2010). Recycling of peroxiredoxin IV provides a novel pathway for disulphide formation in the endoplasmic reticulum. EMBO J 29, 4185–4197.
Tien AC, Rajan A, Schulze KL, Ryoo HD, Acar M, Steller H, Bellen HJ (2008). Ero1L, a thiol oxidase, is required for Notch signaling through cysteine bridge formation of the Lin12-Notch repeats in *Drosophila melanogaster*. J Cell Biol 182, 1113–1125.
Tu BP, Ho-Schleyer SC, Travers KJ, Weissman JS (2000). Biochemical basis of oxidative protein folding in the endoplasmic reticulum. Science 290, 1571–1574.
Tu BP, Weissman JS (2002). The FAD- and O(2)-dependent reaction cycle of Ero1-mediated oxidative protein folding in the endoplasmic reticulum. Mol Cell 10, 983–994.
van Lith M, Tiwari S, Pediani J, Milligan G, Bulleid NJ (2011). Real-time monitoring of redox changes in the mammalian endoplasmic reticulum. J Cell Sci 124, 2349–2356.
Wajih N, Hutson SM, Wallin R (2007). Disulfide-dependent protein folding is linked to operation of the vitamin K cycle in the endoplasmic reticulum. A protein disulfide isomerase-VKORC1 redox enzyme complex appears to be responsible for vitamin K1 2,3-epoxide reduction. J Biol Chem 282, 2626–2635.
Wajih N, Sane DC, Hutson SM, Wallin R (2005). Engineering of a recombinant vitamin K-dependent gamma-carboxylation system with enhanced gamma-carboxyglutamic acid forming capacity: evidence for a functional CXXC redox center in the system. J Biol Chem 280, 10540–10547.
Wang L, Zhu L, Wang CC (2011). The endoplasmic reticulum sulfhydryl oxidase Ero1beta drives efficient oxidative protein folding with loose regulation. Biochem J 434, 113–121.
Wang Y, Zhen Y, Shi Y, Chen J, Zhang C, Wang X, Yang X, Zheng Y, Liu Y, Hui R (2005). Vitamin k epoxide reductase: a protein involved in angiogenesis. Mol Cancer Res 3, 317–323.
Zito E, Chin KT, Blais J, Harding HP, Ron D (2010a). ERO1-beta, a pancreas-specific disulfide oxidase, promotes insulin biogenesis and glucose homeostasis. J Cell Biol 188, 821–832.
Zito E, Melo EP, Yang Y, Wahlander A, Neubert TA, Ron D (2010b). Oxidative protein folding by an endoplasmic reticulum-localized peroxiredoxin. Mol Cell 40, 787–797.